Patterns of coordinated cortical remodeling during adolescence and their associations with functional specialization and evolutionary expansion

Aristeidis Sotiras[a,b,1], Jon B. Toledo[a,c,d], Raquel E. Gur[e], Ruben C. Gur[e], Theodore D. Satterthwaite[a,e,2], and Christos Davatzikos[a,b,2]

[a]Center for Biomedical Image Computing and Analytics, Perelman School of Medicine, University of Pennsylvania, Philadelphia, PA 19104; [b]Department of Radiology, Section of Biomedical Image Analysis, Perelman School of Medicine, University of Pennsylvania, Philadelphia, PA 19104; [c]Department of Pathology and Laboratory Medicine, Perelman School of Medicine, University of Pennsylvania, Philadelphia, PA 19104; [d]Department of Neurology, Houston Methodist Neurological Institute, Houston, TX 77030; and [e]Department of Psychiatry, Neuropsychiatry Section and the Brain Behavior Laboratory, Perelman School of Medicine, University of Pennsylvania, Philadelphia, PA 19104

Edited by Marcus E. Raichle, Washington University in St. Louis, St. Louis, MO, and approved February 3, 2017 (received for review December 30, 2016)

During adolescence, the human cortex undergoes substantial remodeling to support a rapid expansion of behavioral repertoire. Accurately quantifying these changes is a prerequisite for understanding normal brain development, as well as the neuropsychiatric disorders that emerge in this vulnerable period. Past accounts have demonstrated substantial regional heterogeneity in patterns of brain development, but frequently have been limited by small samples and analytics that do not evaluate complex multivariate imaging patterns. Capitalizing on recent advances in multivariate analysis methods, we used nonnegative matrix factorization (NMF) to uncover coordinated patterns of cortical development in a sample of 934 youths ages 8–20, who completed structural neuroimaging as part of the Philadelphia Neurodevelopmental Cohort. Patterns of structural covariance (PSCs) derived by NMF were highly reproducible over a range of resolutions, and differed markedly from common gyral-based structural atlases. Moreover, PSCs were largely symmetric and showed correspondence to specific large-scale functional networks. The level of correspondence was ordered according to their functional role and position in the evolutionary hierarchy, being high in lower-order visual and somatomotor networks and diminishing in higher-order association cortex. Furthermore, PSCs showed divergent developmental associations, with PSCs in higher-order association cortex networks showing greater changes with age than primary somatomotor and visual networks. Critically, such developmental changes within PSCs were significantly associated with the degree of evolutionary cortical expansion. Together, our findings delineate a set of structural brain networks that undergo coordinated cortical thinning during adolescence, which is in part governed by evolutionary novelty and functional specialization.

MRI | cortical thickness | development | nonnegative matrix factorization | cortical organization

The human brain undergoes a protracted course of development throughout adolescence and young adulthood (1), allowing the emergence of cognitive ability and diversification of the behavioral repertoire. However, such plastic change may also confer vulnerability to neuropsychiatric illnesses, which frequently emerge during this critical period. Thus, understanding normal patterns of brain development is necessary for accounts of both healthy maturation and psychopathology. Substantial prior work using structural MRI has documented an early increase in gray matter (2), followed by spatially heterogeneous cortical thinning (3–8). Previous data also suggest that the developmental sequencing of cortical thinning may carry functional significance rooted in evolutionary hierarchy, with lower-order somatomotor cortex maturing before higher-order association areas (4, 9).

The brain is increasingly modeled as a highly networked system, but most prior studies of structural brain maturation have considered the cortex as a set of independent regions using mass-univariate analyses. Prior work has examined developmental change within selected regions (1, 3, 4, 8), across gyri using coarse anatomic atlases (6–8, 10), or with higher-resolution voxelwise analysis (4, 5). However, few efforts have modeled the complete multivariate patterns of structural maturation, which could reveal coordinated development of structural brain networks. Studies have typically used seed-based correlation analyses (11), which are limited to specific locations defined a priori, or have used straightforward clustering techniques (12) that prioritize the mutual exclusion of features, thus not allowing for participation of cortex in multiple networks driven by concurrent processes. Moreover, the degree to which developing structural networks align with large-scale functional networks remains sparsely investigated, with most prior accounts finding little similarity between the two (12). Finally, despite frequent discussion of its relevance, previous studies have not attempted to

Significance

During adolescence, the human cortex is morphed under the influence of regionally heterogeneous and heterochronous processes. Accurately mapping these processes and quantifying their effect is essential for understanding brain development, both in order and disorder. Currently, our understanding remains fundamentally "localizational" in nature, while often being limited by small samples. Here, we capitalize on a large cohort of youths and apply advanced multivariate analysis techniques to capture the coordinated growth of structural brain networks during adolescence. Our results delineate a representation of cortical organization that differs markedly from typical anatomical atlases. This representation comprises structural networks that relate closely to functional brain networks, while exhibiting differential developmental effects that are consistent with an evolutionary view of development.

Author contributions: A.S., T.D.S., and C.D. designed research; A.S. performed research; J.B.T., R.E.G., and R.C.G. contributed new reagents/analytic tools; A.S., T.D.S., and C.D. analyzed data; and A.S., J.B.T., R.E.G., R.C.G., T.D.S., and C.D. wrote the paper.

The authors declare no conflict of interest.

This article is a PNAS Direct Submission.

Data deposition: The data reported in this paper have been deposited in the Database of Genotypes and Phenotypes (dbGaP), www.ncbi.nlm.nih.gov/gap (accession no. phs000607.v1.p1), and in the GitHub repository at https://github.com/asotiras/stable_projects/tree/master/brain_parcellation/Sotiras2017_PNC_CT_NMF.

[1]To whom correspondence should be addressed. Email: aristeidis.sotiras@uphs.upenn.edu.

[2]T.D.S. and C.D. contributed equally to this work.

This article contains supporting information online at www.pnas.org/lookup/suppl/doi:10.1073/pnas.1620928114/-/DCSupplemental.

quantitatively relate developmental changes within structural brain networks to evolutionary cortical expansion (9).

We tested the hypothesis that the cortex matures through the development of spatially heterogeneous, yet regionally coordinated, structural networks. We predicted that structural networks would align with known functional networks and that structural networks would show differential patterns of developmental change based on their evolutionary novelty. To address this hypothesis, we capitalized on a large sample of youth of the Philadelphia Neurodevelopmental Cohort (PNC) (13) and leveraged advances in unsupervised multivariate analysis. Specifically, we delineated structural networks using nonnegative matrix factorization (NMF), which has been highly successful in analyzing diverse types of complex data (14, 15), but has only recently been adapted for use in high-dimensional neuroimaging data (16). NMF allows structural brain networks to be described in a hypothesis-free, data-driven way by identifying complex multivariate patterns of covariation in the data. In contrast to alternative techniques, such as principal components analysis and independent components analysis, which yield widely distributed components with both positive and negative weights that are often difficult to interpret, NMF produces a sparse, parts-based representation of the data.

Using this approach, we derived a set of neurobiologically meaningful patterns of structural covariance (PSCs). As described below, these structural networks are highly reproducible and diverge substantially from traditional gyral-based atlases. They show a correspondence with functional brain networks that is inversely related to functional complexity and demonstrate differential, sex-specific developmental changes during adolescence. Finally, we demonstrate that developmental effects within structural networks are governed in part by each network's position in the evolutionary hierarchy.

Results

We studied a sample of 934 healthy participants aged 8–20 y old, who were imaged as part of the PNC (13). The structural data were processed by using the FreeSurfer software suite (17) to generate cortical-thickness maps. Cortical-thickness maps were analyzed by using NMF (16) to delineate coherent PSCs during development.

NMF Identifies Structural Networks That Are Highly Reproducible. Split-half reproducibility analysis (*SI Appendix*, Fig. S1) and reconstruction error analysis (*SI Appendix*, Fig. S2) were used to examine network resolutions ranging from 2 to 60 PSCs. The reproducibility analysis demonstrated that stability was not uniform; as expected, reproducibly declined as network resolution increased. However, clear peaks of reproducibility occurred for the 2-, 7-, and 18-PSC solutions (Fig. 1), which were explored further. Across split-half folds, identified networks were often qualitatively impossible to distinguish (Fig. 1 and *SI Appendix*, Fig. S3), emphasizing the robustness of the networks identified by the decomposition. Despite this method being completely unsupervised and data-driven, nearly all PSCs were highly symmetric bilaterally, regardless of the resolution of the decomposition. The 2-PSC solution identified an anterior–posterior division of the cortex (*SI Appendix*, Fig. S4). This division followed the central sulcus closely, separating frontal, temporal, and inferior parietal cortices (anterior PSC) from occipital and superior parietal cortices (posterior PSC). In the 7-PSC solution (*SI Appendix*, Fig. S5), anterior cortex was subdivided into anterior and middle temporal lobe. Notably, one PSC was composed of cortex that recapitulates the large-scale functional network known as the frontoparietal control network (FPN; PSC 5 in *SI Appendix*, Fig. S5) (18, 19). When these networks were further divided as part of the 18-PSC solution (Fig. 2 and *SI Appendix*, Figs. S6 and S7), reproducibility remained high, while better reconstruction was

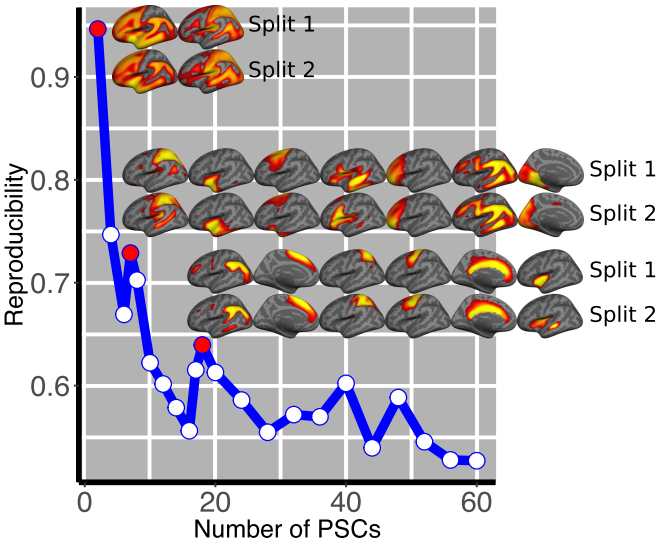

Fig. 1. Reproducibility of the decomposition algorithm is plotted as a function of the estimated patterns for the split-half analysis. The decomposition is less stable with increasing number of estimated PSCs, which is expected because the complexity of the problem increases, while the size of the patterns and the modeled effect decreases. The local maxima (marked by color-filled circles) indicate the number of patterns that can be stably estimated (i.e., 2, 7, and 18 patterns). Indicative views of the estimated patterns across splits are also shown (for the 18-PSC solution, see also *SI Appendix*, Fig. S3).

achieved. As noted above, even at the relatively higher resolution provided by 18 PSCs, most networks were remarkably symmetric. Two notable exceptions were language-related PSCs that closely approximated Wernicke's (PSC 7) and Broca's (PSC 18) area, respectively. Moving forward, we focus on the 18-PSC solution.

PSCs Correspond to Known Functional Networks and Are Functionally Coherent. Many of the PSCs appeared to demonstrate a notable correspondence to known large-scale functional networks. To explicitly test the relationship between PSCs and functional networks, we compared the PSCs to the widely used 7-network functional parcellation of Yeo et al. (18) (*SI Appendix*, Fig. S8; for convergent results using the 17-network parcellation of Yeo et al., see *SI Appendix*, Fig. S9). Correspondence between functional and structural networks was assessed by using the inner product of their spatial distribution (*SI Appendix*, Fig. S10, *Upper*), with the significance determined by using permutation testing (*SI Appendix*, Fig. S10, *Lower*). The correspondence between PSCs and known functional systems was prominent in lower-order functional networks (Fig. 3; also see *SI Appendix*, Fig. S10) and diminished according to an evolutionary hierarchy of cortical expansion and cognitive complexity. Most dramatically, much of the visual functional network was captured by a single structural network (PSC 4; also see *SI Appendix*, Fig. S11). In the 7-network parcellation provided by Yeo et al., primary motor, somatosensory, and auditory cortices are represented as a single functional network. These three separate functional systems are represented by distinct PSCs, with separate bilaterally symmetric patterns being found for each element (motor, PSC 8; somatosensory, PSC 11; and auditory, PSC 7; also see *SI Appendix*, Fig. S12). Similarly, the third PSC comprised almost entirely cortex belonging to the limbic functional network (also see *SI Appendix*, Fig. S13).

Although not as dramatic as in lower-order brain regions, several PSCs displayed a strong correspondence to the dorsal and ventral attention systems. Superior parietal cortex of the dorsal attention system overlapped mainly with PSC 6 (*SI Appendix*, Fig. S14). Bilateral insular cortex was encompassed entirely by PSC

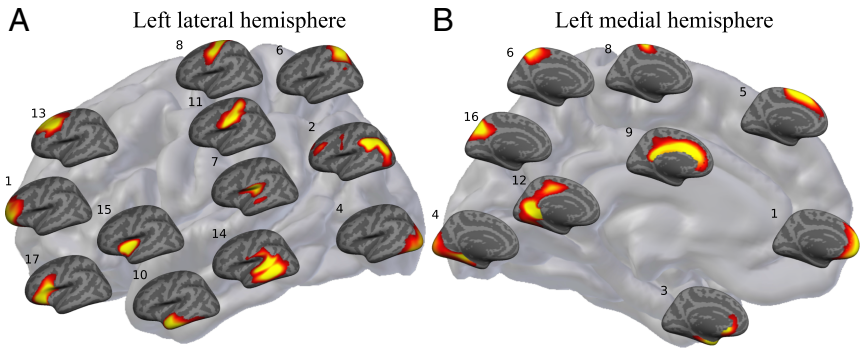

Fig. 2. A grid placement of the 18-PSC solution on the lateral (*A*) and medial (*B*) aspect of the left cortical hemisphere (for the right cortical hemisphere, see *SI Appendix*, Fig. S7). The location of each PSC on the gray brain map represents the location each component best encodes. Warmer colors correspond to higher values. In describing the estimated PSCs, we use conventional anatomical labels, but these only approximate the observed patterns: 1, prefrontal cortex (PFC); 2, inferior lateral parietal cortex; 3, entorhinal cortex and medial temporal pole; 4, occipital cortex; 5, superior frontal cortex; 6, superior parietal cortex; 7, perisylvian region; 8, primary motor cortex; 9, cingulate; 10, inferior and anterior middle temporal lobe; 11, primary somatosensory cortex; 12, lingual gyrus; 13, dorsolateral frontal cortex; 14, left posterior middle and superior temporal lobe; 15, insula; 16, precuneus; 17, inferior frontal cortex; and 18, pars opercularis and triangularis predominantly present in the right hemisphere (not shown here; *SI Appendix*, Fig. S7).

15 and showed significant overlap with that element of the ventral attention (cingulo-opercular) system (*SI Appendix*, Fig. S15). The FPN and the default mode network (DMN) are generally considered to subserve the most complex cognitive functions, and they have the highest degree of areal expansion in humans compared with macaques. In sharp contrast to lower-order systems, where there was strong correspondence between PSCs and functional networks, we did not observe significant overlap between these two large-scale functional networks (*SI Appendix*, Fig. S10). Instead, these networks seemed decomposed into multiple PSCs that sometimes had substantial overlap across networks (e.g., frontopolar cortex in PSC 1 and lateral PFC in PSC 13). However, several PSCs had relatively specific loading onto the DMN, but not the FPN (PSCs 10 and 14). Lastly, although components in the 18-PSC solution did not comprise long-range relations (apart from interhemispheric ones), components of the 2- and 7-PSC solutions did. The anterior–posterior division (2-PSC solution) bore certain similarities to the two-system (intrinsic–extrinsic) solution reported by Golland et al. (20). Similar to the intrinsic functional network, our anterior network grouped together frontal, inferior parietal, and inferior temporal cortices, whereas, similar to the extrinsic functional network, our posterior network comprised mainly auditory, visual, and somatosensory cortices. Furthermore, one component in the 7-PSC solution did show a striking correspondence to the FPN (*SI Appendix*, Fig. S5).

The above analyses demonstrate correspondence between specific lower-order PSCs and known large-scale functional networks. To further study the functional relevance of structural covariance, we investigated the functional coherence of structural PSCs in a subsample of 524 participants, who also completed resting-state functional connectivity (rsfc-MRI) imaging (*SI Appendix*, Fig. S16). The appropriateness of the structurally derived functional parcellation was evaluated by using a quality index compared with a null distribution from spatial permutations that preserved local autocorrelation. This procedure established that structurally derived PSCs demonstrated significant functional coherence ($FPQI = 9.84,\ p = 0.006$; see also *SI Appendix*, Fig. S17). When each PSC was evaluated individually, visual (PSC 4, $p = 0.005$) and motor (PSC 11, $p = 0.017$) had elevated intraparcel functional coherence, providing convergent evidence for the strong correspondence between structure and lower-order functional networks.

PSCs Display Differential Developmental Effects. The data-driven NMF approach identified patterns of covariance in this large developmental sample, but did not include information regarding participant age or sex. Accordingly, we next investigated whether males and females exhibited developmental differences (*SI Appendix*, Table S1), and whether developmental patterns varied across the PSCs using stepwise polynomial regression (*SI Appendix*, Table S2); correlations were also performed to estimate effect sizes (*SI Appendix*, Table S3 and Fig. S18). This procedure identified significant sex and sex-by-age interaction effects in frontal cortex (PSCs 5, 13, and 17), cingulate cortex (PSC 9), and parietal cortex (PSCs 2, 7, and 16; *SI Appendix*, *SI Results*), as well as linear and quadratic developmental effects (*SI Appendix*, Fig. S19). Despite the unbiased decomposition used, PSCs showed heterogeneous associations with age, with effect sizes ranging from small (PSC 3: $r = -0.19$) to large (PSC 12: $r = -0.66$).

To compactly summarize both mean thickness and developmental effects, we plotted mean PSC thickness (regression intercept) vs. the linear developmental slope (Fig. 4). Several of the

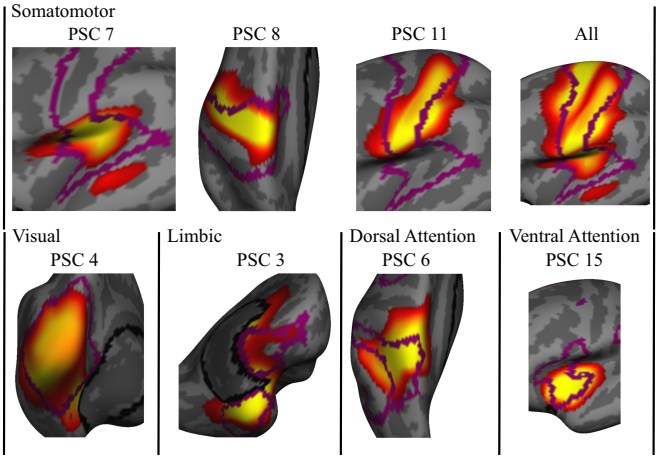

Fig. 3. Close-up of the overlap between functional networks (18) and best corresponding PSCs (statistically significant results at false discovery rate level 0.05). Borders of functional networks are shown as purple lines. The somatomotor functional network overlaps strongly with three PSCs: the 7th, 8th, and 11th PSCs (approaching statistical significance). The visual network shows strong alignment with the 4th PSC, whereas the limbic network corresponds largely to the 3rd PSC. Dorsal and ventral attention functional networks align well with the 6th and 15th PSCs, respectively. High-order distributed FPN and DMN were not coupled with a specific PSC.

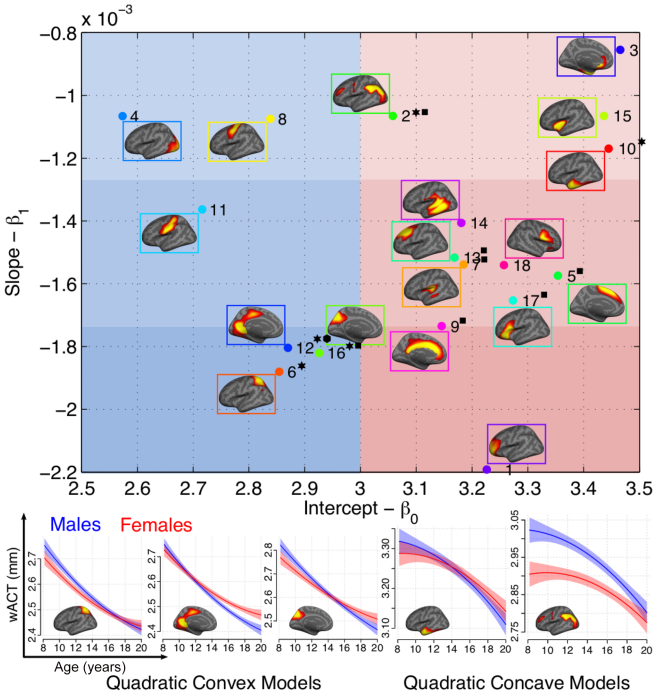

Fig. 4. Scatter plot of the estimated linear model regression coefficients for each PSC (the *x* and *y* axes indicate the intercept and slope values, respectively). Star denotes best-fitting quadratic model; respective models are shown for males (blue) and females (red) in *Lower*. A square denotes significant sex and sex-by-age interaction effects, and a hexagon denotes only significant sex-by-age interaction effect. The points for different PSCs are color-coded by distinct colors. Characteristic views of the corresponding PSCs are shown next to the respective points, enclosed by a bounding box of the same color as the point. The figure is color-partitioned to low–high cortical thickness (blue corresponds to low values) and to low, moderate, and steep slope (darker colors correspond to steeper slope values).

thinnest regions had only limited developmental effects. For example, PSCs in the visual cortex (PSC 4) and precentral cortex (PSC 8) were both thin and had limited developmental changes during the age range sampled. Conversely, prefrontal regions, including the anterior PFC (PSC 1), medial frontal cortex (PSC 5), cingulate cortex (PSC 9), dorsolateral PFC (PSC 13), and inferior frontal gyrus (PSC 17), all showed dramatic developmental effects within cortex that is, on average, thicker during the age range examined. Together, these results delineate cortical organization in adolescence by concisely summarizing both cortical topography and associated age-related variation. Furthermore, the ordering of developmental effects from lower order (i.e., primary visual and somatomotor) to higher order (frontal association cortex) suggests that developmental effects may be in part linked to evolutionary novelty.

Developmental Patterns of Cortical Thinning Are Governed in Part by Evolutionary Expansion. To test whether developmental effects are linked to evolutionary novelty, we examined how evolutionary expansion of the cortex was associated with both mean PSC thickness and observed developmental effects. By using a published atlas of cortical expansion (9), cortical expansion was averaged within each PSC (Fig. 5*C*). Critically, evolutionary expansion was associated with both mean cortical thickness ($r = 0.6$, $p < 0.01$; Fig. 5*D*) and the linear slope of age effects ($r = -0.62$, $p = 0.032$; Fig. 5*E*). Thus, regions with greater evolutionary expansion both were thicker and exhibited greater developmental changes during adolescence. Finally, although the small number of PSCs precluded statistical testing, regions that displayed significant quadratic age effects (Fig. 4, *Lower*) showed differences in evolutionary expansion according to whether the quadratic effect was concave or convex. Specifically, late-developing PSCs with concave developmental patterns showed a high level of cortical expansion compared with early developing regions with a convex pattern (Fig. 5*F*). Correspondence with evolutionary expansion was also observed for the 2-PSC solution (Fig. 5*B*), as well as for vertexwise developmental data (*SI Appendix*, *SI Results*).

Discussion

We used advanced multivariate methods in a large cohort of youth to capture the coordinated growth of structural brain networks during adolescence. These networks differ substantially from typical anatomical atlases, and instead align with functional brain networks in a way that diminishes with increasing functional complexity and developmental remodeling. Critically, these developmental changes are driven in part by each network's position in the evolutionary hierarchy of cortical expansion. Together, these results delineate a representation of cortical organization and development.

Topography of Coordinated Cortical Development. We used NMF to decompose the cortex into covariance-based structural networks exhibiting coordinated development. Notably, identified networks were highly reproducible at multiple scales. In deriving this reproducible structural representation of the cortex, four features of the hypothesis-free, data-driven methodological approach were crucial. First, even without a hierarchical constraint, higher resolutions demonstrated increasing differentiation, while largely respecting the boundaries of coarser subdivisions. This effect is consistent with an economical cortical organization (21) that is implemented in a hierarchical way, where small morphogenetic differences accrue across scales, leading to the emergence of functionally specialized units. Second, without incorporating any constraint for spatial contiguity and sparsity, the decomposition revealed sparse patterns that exhibit high spatial contiguity within hemispheres. Importantly, these patterns neither form blobs, which could arise from smoothing imaging data, nor are driven by spatial proximity alone. Thus, our results further support evidence for small-world, functionally driven network properties in human brain cortical gray matter structure (22, 23). Third, our approach is blind to location in space and was conducted on both hemispheres simultaneously, with no constraint for hemispheric symmetry. Still, the majority of derived PSCs were predominantly symmetric bilaterally. However, hemispheric asymmetries were observed in regions such as Broca's and Wenicke's areas, where lateralization is expected. Fourth and finally, our analysis is agnostic to genetic or anatomical priors. Nonetheless, the identified components corresponded closely to meaningful genetic (24) and structural units (Fig. 2 and *SI Appendix*, Fig. S7). Specifically, they showed close relatedness to genetic patterning of cortical thickness (12-cluster solution of ref. 24), which is consistent with recent results showing that genetic factors affect cortical changes throughout life (25). Additionally, despite similarity to structural units, they differed markedly from common atlas definitions. The estimated PSCs did not necessarily follow gyral boundaries (e.g., anterior–posterior division of temporal cortex in PSCs 10 and 14). Moreover, cortical elements participated in multiple networks, potentially driven by concurrent processes.

Functional Relevance of Structural Covariance. Prior studies have sought to map structural covariance networks to functional networks, but have produced mixed results. Although seed-based analyses of selected regions have demonstrated overlap with functional patterns (11, 26), previous whole-brain covariance-based parcellations have not aligned well with known large-scale

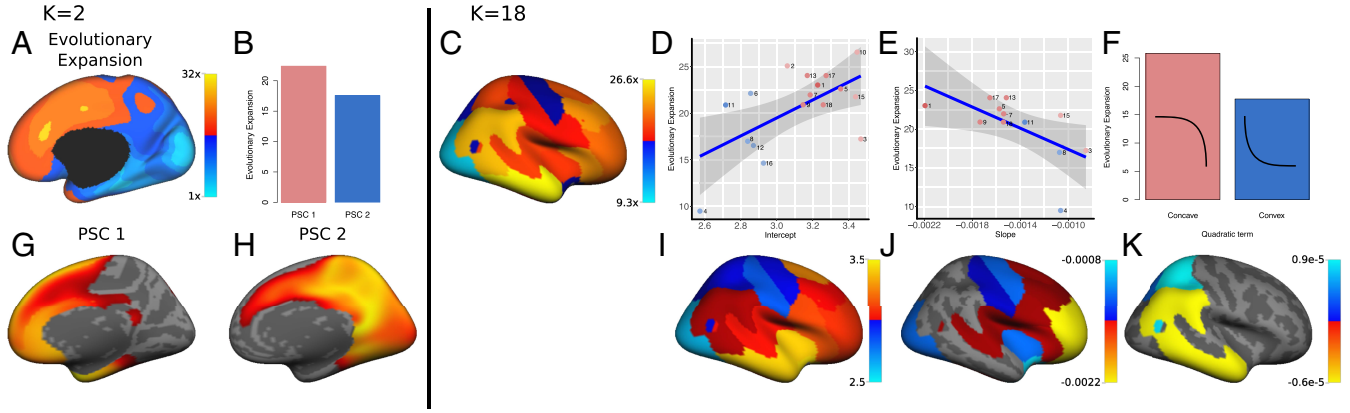

Fig. 5. (*Left*) Relationship between evolutionary novelty and 2-PSC solution. (*A*) Cortical expansion (9). (*B*) Average cortical expansion within first (shown in *G*) and second PSC (shown in *H*). (*Right*) Relationship between evolutionary novelty and developmental effects for the 18-PSC solution. (*C*) Average cortical expansion within each PSC. Associations of cortical expansion with: (*D*) average cortical thickness, or intercept (shown in *I*); (*E*) cortical thickness change, or slope (shown in *J*); and (*F*) quadratic effects (shown in *K*). Warmer colors in colormaps correspond to regions of higher evolutionary expansion. Points in regression plots are color-coded according to the color partition of Fig. 4.

functional networks (12, 27). In contrast to these prior efforts, the PSCs produced by NMF showed significant overlap with certain functional networks. This correspondence was present in both a parcellation derived from an independent dataset and when using functional imaging data from a subset of our participants. Notably, the convergence between PSCs and functional networks was inversely related to functional complexity. Motor, sensory, visual, and limbic functional networks aligned to distinct PSCs. This correspondence may be due to the high specialization and old evolutionary age of these networks. Functional specialization may impose constraints on the determinants of regional cortical thickness, while the evolutionary preservation may have allowed genes influencing these regions to reach allelic fixation, as suggested by low genetic variability in these areas (28, 29). Together, these factors may explain the high coordination and low intersubject variance in these regions (30). This finding emphasizes the distinct, specialized nature of low-order networks that develop in a segregated fashion. Conversely, functional and structural correspondence in higher-order networks was less apparent. The link between structure and function may be weakened by relatively high levels of interindividual variability within these functional complex networks (31, 32), which has been emphasized by recent studies of individual difference in cortical neuroanatomy (33, 34). One exception to the weak correspondence between PSCs and higher-order networks is the recapitulation of the FPN seen in the 7-PSC solution, emphasizing that structure–function relationships require evaluation at multiple scales.

Cortical Patterning, Maturation Timing, and Evolutionary Hierarchy. Although the spatial decomposition of the cortex was agnostic to age and sex, the derived components demonstrated markedly different developmental patterns. As in prior reports, we found that mean cortical thickness in males was initially greater than that in females throughout most of the association cortex [an effect that was inverted at 20 y (35)] and that primary motor and somatosensory networks mature before higher-order association cortices (4, 5). Thus, PSCs mapping to sensorimotor cortices were associated with small age effects, whereas PSCs within higher-order association cortex exhibited greater developmental changes. Critically, such variation in the developmental effects of these structural networks aligned well with data regarding evolutionary cortical expansion. Structural networks with greater evolutionary expansion were both thicker and exhibited greater developmental change during adolescence, consistent with greater functional complexity in adulthood (9) and protracted maturation (1, 4, 5). Notably, our 2-PSC solution exemplifies this distinction, aligning remarkably with regional evolutionary cortical expansion (9); the anterior PSC encoded regions of high expansion, whereas the posterior PSC encoded regions of low expansion (*SI Appendix*, Fig. S20).

Limitations. Although this study capitalized on a large sample and advanced methods, certain limitations should be noted. First, our inferences on cortical development are drawn from cross-sectional data; longitudinal data may provide superior estimates of cortical development. However, the multivariate nature of our analysis largely overcomes this limitation by leveraging contrasts among different brain regions, rather than against a baseline measure. Second, primary somatosensory regions may have undergone substantial maturation at the lower end of the age range in our cohort (4, 5). Third, although associations between structural components and both functional networks as well as evolutionary expansion are suggestive and intuitive, such correlational analyses do not establish causality. Lastly, our analysis draws only from cortical-thickness data, thus not exploiting complementary information from other modalities that could lead to better elucidating concurrent developmental processes (36).

Study Implications. Despite these limitations, the identified networks have the potential to become an important alternative to existing atlas definitions (36), providing a concise summary of the data that will facilitate integration with other high-dimensional data types (e.g., genomics). Additionally, being informed by specific neurodevelopmental data, they enable further studies to understand how they support cognitive abilities that develop during this epoch and provide an important context for understanding how abnormal development is associated with psychopathology (37). Lastly, our methodological framework is general and fully automatic and can be readily applied to other datasets.

Conclusions

Our study provides insights into cortical organization and maturation during adolescence. We demonstrated that cortical development progresses in a spatially heterogeneous fashion by integrating highly coordinated units. These structural networks mirrored both certain functional networks and the evolutionary expansion of the cerebral cortex and could provide a concise and effective representation of cortical structure and maturation.

Materials and Methods

Participants and Neuroimaging. All participants were imaged as part of the PNC (13). All subjects, or their parent or guardian, provided informed consent, and minors provided assent; study procedures were approved by the institutional review boards of both the University of Pennsylvania and the Children's Hospital of Philadelphia. All included participants were medically healthy, were not taking psychotropic medication, and had imaging data that passed strict quality-assurance procedures. The final sample included 934 youths (512 males) ages 8–20 (mean, 14.44 y; SD, 3.24). A subsample of 524 youth also completed rsfc-MRI imaging (215 males; mean age 15.45; SD 2.86). For further details, see *SI Appendix, SI Methods*.

Multivariate Analysis of Structural Covariance. PSCs were estimated by using NMF (14, 16), which factors the data by positively weighting cortical elements that covary. This method leads to a highly specific and reproducible (*SI Appendix, SI Results*) parts-based representation, where parts are combined in an additive way to form a whole. Model selection was performed by using split-sample reproducibility analysis and evaluation of the reconstruction quality. For further details, see *SI Appendix, SI Methods*.

Estimation of Structure–Function Associations. We studied the functional relevance of structural covariance by using the inner product (range 0–1) to examine the overlap between the estimated PSCs and functional clusters estimated in an independent cohort of 1,000 subjects (18) (*SI Appendix*, Fig. S8). The functional coupling of the estimated PSCs was further evaluated by assessing the appropriateness of a PSC-derived parcellation to fit the available rsfc-MRI scans. The goodness of fit was summarized by a functional parcellation quality index (FPQI) that collectively evaluated the functional compactness and separation of the parcels; intraparcel and interparcel coherence were evaluated as well. Statistical significance was evaluated by using permutation testing (38). For further details, see *SI Appendix, SI Methods*.

Analysis of Developmental Effects and Evolutionary Expansion. Age-related effects were modeled for each PSC by using stepwise polynomial regression including sex and sex-by-age interaction terms; inclusion of quadratic terms was evaluated by using Akaike information criterion (8). The effect size of the linear term for each PSC was determined by using Pearson's correlation. To describe the relationship between the mean cortical thickness of each PSC and observed developmental effects, we plotted the coefficient of the model intercept (mean thickness) vs. the coefficient of the linear age term (developmental slope). Finally, we evaluated whether developmental changes of each PSC showed an association with the evolutionary expansion of the cortex, using a published atlas of cortical surface area expansion (9). Expansion was calculated for each PSC, and associations between expansion and both mean thickness and developmental effects were described by using Pearson's correlations. The expansion of PSCs with convex and concave quadratic effects was compared for the PSCs with a significant quadratic term. For further details, see *SI Appendix, SI Methods*.

ACKNOWLEDGMENTS. This work was supported by National Institute of Mental Health Grants MH107235, MH089983, MH089924, MH096891, MH101111, and MH107703; National Institute of Biomedical Imaging and Bioengineering Grant EB022573; National Institute of Neurological Disorders and Stroke Grant NS042645; and the Dowshen Program for Neuroscience.

1. Toga AW, Thompson PM, Sowell ER (2006) Mapping brain maturation. *FOCUS* 4(3): 378–390.
2. Knickmeyer RC, et al. (2008) A structural MRI study of human brain development from birth to 2 years. *J Neurosci* 28(47):12176–12182.
3. Sowell ER, et al. (2004) Longitudinal mapping of cortical thickness and brain growth in normal children. *J Neurosci* 24(38):8223–8231.
4. Gogtay N, et al. (2004) Dynamic mapping of human cortical development during childhood through early adulthood. *Proc Natl Acad Sci USA* 101(21):8174–8179.
5. Shaw P, et al. (2008) Neurodevelopmental trajectories of the human cerebral cortex. *J Neurosci* 28(14):3586–3594.
6. Tamnes CK, et al. (2010) Brain maturation in adolescence and young adulthood: Regional age-related changes in cortical thickness and white matter volume and microstructure. *Cereb Cortex* 20(3):534–548.
7. Group BDC (2012) Total and regional brain volumes in a population-based normative sample from 4 to 18 years: The NIH MRI study of normal brain development. *Cereb Cortex* 22(1):1–12.
8. Taki Y, et al. (2013) Linear and curvilinear correlations of brain gray matter volume and density with age using voxel-based morphometry with the Akaike information criterion in 291 healthy children. *Hum Brain Mapp* 34(8):1857–1871.
9. Hill J, et al. (2010) Similar patterns of cortical expansion during human development and evolution. *Proc Natl Acad Sci USA* 107(29):13135–13140.
10. Lenroot RK, et al. (2007) Sexual dimorphism of brain developmental trajectories during childhood and adolescence. *Neuroimage* 36(4):1065–1073.
11. Zielinski BA, Gennatas ED, Zhou J, Seeley WW (2010) Network-level structural covariance in the developing brain. *Proc Natl Acad Sci USA* 107(42):18191–18196.
12. Krongold M, Cooper C, Bray S (December 9, 2015) Modular development of cortical gray matter across childhood and adolescence. *Cereb Cortex*, 10.1093/cercor/bhv307.
13. Satterthwaite TD, et al. (2014) Neuroimaging of the Philadelphia neurodevelopmental cohort. *Neuroimage* 86:544–553.
14. Seung HS, Lee DD (1999) Learning the parts of objects by non-negative matrix factorization. *Nature* 401(6755):788–791.
15. Brunet JP, Tamayo P, Golub TR, Mesirov JP (2004) Metagenes and molecular pattern discovery using matrix factorization. *Proc Natl Acad Sci USA* 101(12):4164–4169.
16. Sotiras A, Resnick SM, Davatzikos C (2015) Finding imaging patterns of structural covariance via non-negative matrix factorization. *Neuroimage* 108:1–16.
17. Fischl B (2012) FreeSurfer. *Neuroimage* 62:774–781.
18. Yeo BTT, et al. (2011) The organization of the human cerebral cortex estimated by intrinsic functional connectivity. *J Neurophysiol* 106(3):1125–1165.
19. Dosenbach NUF, et al. (2007) Distinct brain networks for adaptive and stable task control in humans. *Proc Natl Acad Sci USA* 104(26):11073–11078.
20. Golland Y, Golland P, Bentin S, Malach R (2008) Data-driven clustering reveals a fundamental subdivision of the human cortex into two global systems. *Neuropsychologia* 46(2):540–553.
21. Bullmore E, Sporns O (2012) The economy of brain network organization. *Nat Rev Neurosci* 13(5):336–349.
22. He Y, Chen ZJ, Evans AC (2007) Small-world anatomical networks in the human brain revealed by cortical thickness from MRI. *Cereb Cortex* 17(10):2407–2419.
23. Bassett DS, et al. (2008) Hierarchical organization of human cortical networks in health and schizophrenia. *J Neurosci* 28(37):9239–9248.
24. Chen CH, et al. (2013) Genetic topography of brain morphology. *Proc Natl Acad Sci USA* 110(42):17089–17094.
25. Fjell AM, et al. (2015) Development and aging of cortical thickness correspond to genetic organization patterns. *Proc Natl Acad Sci USA* 112(50):15462–15467.
26. Raznahan A, et al. (2011) Patterns of coordinated anatomical change in human cortical development: A longitudinal neuroimaging study of maturational coupling. *Neuron* 72(5):873–884.
27. Alexander-Bloch A, Raznahan A, Bullmore E, Giedd J (2013) The convergence of maturational change and structural covariance in human cortical networks. *J Neurosci* 33(7):2889–2899.
28. Lenroot RK, et al. (2009) Differences in genetic and environmental influences on the human cerebral cortex associated with development during childhood and adolescence. *Hum Brain Mapp* 30(1):163–174.
29. Schmitt JE, et al. (2014) The dynamic role of genetics on cortical patterning during childhood and adolescence. *Proc Natl Acad Sci USA* 111(18):6774–6779.
30. Fischl B, Dale AM (2000) Measuring the thickness of the human cerebral cortex from magnetic resonance images. *Proc Natl Acad Sci USA* 97(20):11050–11055.
31. Mueller S, et al. (2013) Individual variability in functional connectivity architecture of the human brain. *Neuron* 77(3):586–595.
32. Langs G, et al. (2015) Identifying shared brain networks in individuals by decoupling functional and anatomical variability. *Cereb Cortex* 26(10):4004–4014.
33. Laumann TO, et al. (2015) Functional system and areal organization of a highly sampled individual human brain. *Neuron* 87(3):658–671.
34. Satterthwaite TD, Davatzikos C (2015) Towards an individualized delineation of functional neuroanatomy. *Neuron* 87(3):471–473.
35. Raznahan A, et al. (2010) Longitudinally mapping the influence of sex and androgen signaling on the dynamics of human cortical maturation in adolescence. *Proc Natl Acad Sci USA* 107(39):16988–16993.
36. Glasser MF, et al. (2016) A multi-modal parcellation of human cerebral cortex. *Nature* 536(7615):171–178.
37. Paus T, Keshavan M, Giedd JN (2008) Why do many psychiatric disorders emerge during adolescence? *Nat Rev Neurosci* 9:947–957.
38. Gordon EM, et al. (2016) Generation and evaluation of a cortical area parcellation from resting-state correlations. *Cereb Cortex* 26(1):288–303.